

## **SMASIS2018-8005**

### **A CHEMO-MECHATRONIC ORIGAMI DEVICE FOR CHEMICAL SENSING**

#### **Chang Liu**

Expeditionary Robotics Lab  
Mechanical and Industrial Engineering  
Northeastern University  
Boston, Massachusetts 02115  
Email: liu.chang7@husky.neu.edu

#### **Conor M. Gomes**

Biomaterials Design Group  
Chemistry and Chemical Biology  
Northeastern University  
Boston, Massachusetts 02115  
Email: gomes.co@husky.neu.edu

#### **Kevin J. McDonald**

Expeditionary Robotics Lab  
Mechanical and Industrial Engineering  
Northeastern University  
Boston, Massachusetts 02115  
Email: mcdonald.kev@husky.neu.edu

#### **Leila F. Deravi**

Biomaterials Design Group  
Chemistry and Chemical Biology  
Northeastern University  
Boston, Massachusetts 02115  
Email: l.deravi@northeastern.edu

#### **Samuel M. Felton\***

Expeditionary Robotics Lab  
Mechanical and Industrial Engineering  
Northeastern University  
Boston, Massachusetts 02115  
Email: s.felton@northeastern.edu

### **ABSTRACT**

*This paper presents the design, fabrication, and operation of a chemo-mechatronic system that changes its geometry and electrical functionality in the presence of specific chemical signals. To accomplish this, we integrated a protein hydrogel with an aluminum substrate and flexible circuit in a low-profile laminate. To demonstrate the concept, we have built and tested a sensor that lights an LED when actuated in the presence of polyethylene glycol (PEG).*

### **NOMENCLATURE**

PEG Polyethylene Glycol  
PDA Polydopamine

### **INTRODUCTION**

Self-folding is a process in which a flat sheet folds itself along pre-programmed hinges to form a three-dimensional structure. It has been applied to a variety of devices, from meter-

scale robots [1] to micrometer-scale cell-biopsy grippers [2]. It can be used to automate the assembly of multiple machines in parallel [3], construct devices that are too small to manipulate manually [4], and transform machines between different shapes for different locomotion modes [5] [6]. Folding can be actuated with a variety of techniques, including shape memory polymers [7] [8], shape memory alloys [9–13], and pneumatics [14] [15].

One particular type of self-folding uses hydrogel swelling [16]. Hydrogels have a wide range of uses due to their swelling behavior, including biomedical sensors and mechanical parts [17–19]. They can be actuated by thermal reaction [20] or by successive extension of cross-links [21]. Many hydrogels are also bio-compatible and can be used to deliver drugs and other molecules [22]. In this paper we use gelatin [23] from denatured collagen to form a hydrogel [24] [25].

In this paper we present a self-folding sensor that combines an active hydrogel layer with an aluminum scaffold and a copper circuit. The general concept of operation is that a chemical reaction in the hydrogel causes mechanical deformation of the scaffold, which in turn leads to electrical changes in the circuit that can be used to sense the original chemical signal. We first

\*Address all correspondence to this author.

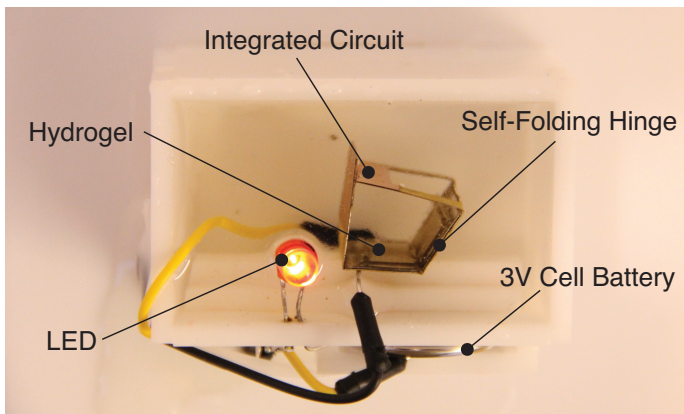


**FIGURE 1:** A SELF-FOLDING SENSOR WITH A CIRCUIT AND EMBEDDED CONDUCTIVE TRACE.

characterized the relationship between the self-folding hinge geometry (hinge thickness and hydrogel thickness) and the fold angle. Then, to demonstrate the efficacy of this concept, we built a device with a self-folding hinge and a circuit with embedded conductive trace including a battery and an LED. The device was partially submerged into PEG for eight hours. The PEG dehydrates the hydrogel and causes it to contract, which in turn causes the hinge to fold. Once the hinge folds, two electrodes on either side of the structure connect and the LED lights up, signaling the presence of PEG. This prototype demonstrates the potential for similar chemo-mechatronic systems, and we expect that this approach could one day be applied to in vivo biosensors, chemical warning systems, and chemically reactive robots.

## DESIGN AND FABRICATION

### Foldable Hinge (Scaffold)

The scaffold was laminated with three layers: two rigid layers and a flexural layer. The rigid layers are 100  $\mu\text{m}$  thick aluminum shims, and the flexural layer is nylon film, either 25  $\mu\text{m}$  and 50  $\mu\text{m}$  thick. The flexural layer was sandwiched between two rigid layers and the laminate was bonded together with high-strength glue-on-a-roll (3M F9460PC). An articulated hinge was created by removing a thin strip of aluminum from either side of the laminate, leaving the nylon exposed and able to bend freely (Fig. 2).

There are seven steps to fabricating the scaffold. First, acrylic was used as a flat base and aluminum shims were stuck to the acrylic using GelPak (WF-60-X4-A) (Fig. 3(a)). By using the acrylic and the GelPak, the aluminum stayed flat during the laser cutting, enabling clean and consistent cuts. The aluminum shims were then cut with the fiber laser cutter (Universal Laser Systems, PLS6MW), using the pre-designed patterns (Fig. 3(b)). Cut aluminum shims were cleaned by sonicating in 70% ethanol

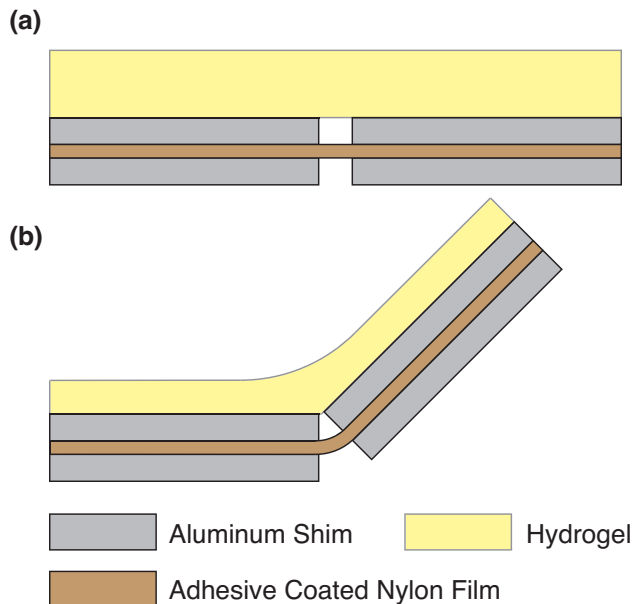


**FIGURE 2:** WORKING PRINCIPLE OF THE SCAFFOLD. (a) FLAT. (b) FOLDED.

for one hour and dried for one hour at 60° (Fig. 3(c)). Another set of acrylic and GelPak was used, and holes were cut for pin alignment (Fig. 3(d)(e)). Then, adhesive coated nylon film was sandwiched between the two cleaned aluminum shims, and the whole assembly was pin-aligned to the base from the previous step (Fig. 3(f)). A release cut was used to cut the desired scaffold from the assembly (Fig. 3(g)).

### Hydrogel

Before attaching the hydrogel, the scaffold was cleaned by sonicating in 70% ethanol for one hour and dried for one hour at 60°C. We used polydopamine (PDA) to attach our hydrogel to a scaffold, since the catechol group within the PDA structure allows spontaneous formation of a covalent bond with gelatin [26] [27]. Gelatin powder (Type A, 300 bloom, Electron Microscopy Sciences) was dissolved in water at 60 °C to achieve 20 wt/v% (weight/volume percent). T1 Transglutaminase Formula (Modernist Pantry) was dissolved in water at 30 °C to achieve a 8 wt/v% solution. The two solutions were mixed 1:1. The hydrogel was pipetted into a mold on top of the scaffold and left to cure for an hour. To increase the mechanical stability and alter the water-diffusion we covalently crosslinked our gelatin hydrogel with transglutaminase [28].

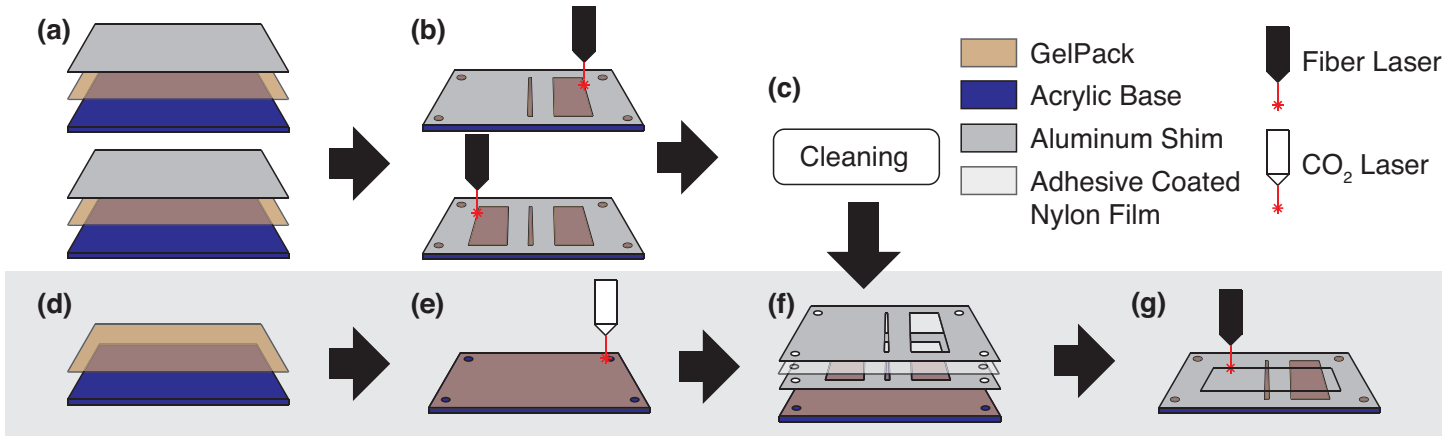


**FIGURE 3:** THE FABRICATION PROCESS FOR SCAFFOLDS. (a) ALUMINUM SHIMS ARE SECURED TO ACRYLIC BASE. (b) SHIMS ARE CUT WITH LAYER-SPECIFIC PATTERNS. (c) SHIMS ARE CLEANED. (d) GELPAK IS APPLIED TO ACRYLIC BASE. (e) ALIGNMENT HOLES ARE CUT. (f) NYLON FILM IS SANDWICHED BETWEEN THE SHIMS. (g) RELEASE CUT IS APPLIED TO PRODUCE THE FINAL SCAFFOLD.

## MODEL

To predict the fold angle of the self-folding hinges, we applied an analytical model that treats the nylon hinge and the hydrogel as a bilayer with asymmetric strain, bounded by the aluminum on either side. Using a generalized version of a method outlined by Timoshenko [29], the final curvature of the bilayer can be determined from the balance of strain longitudinal to the bilayer at the interface between the two layers. Eqn. 1 is a modified version of Timoshenko's Equation 4 with thermal strain replaced with the general form of strain.

$$\rho = \frac{\frac{h}{2} + \frac{2(E_1 I_1 + E_2 I_2)}{hw} \left( \frac{1}{E_1 a_1} + \frac{1}{E_2 a_2} \right)}{\varepsilon_2 - \varepsilon_1} \quad (1)$$

where  $\rho$  is the radius of curvature of the bilayer,  $h$  is the total thickness of the bilayer after dehydration,  $E$  is the Young's modulus of either layer,  $I$  is the moment of inertia of either layer,  $w$  is the width of the bilayer,  $a$  is the thickness of either layer after dehydration as determined experimentally, and  $\varepsilon$  is the free strain in each of the layers due to dehydration. Subscript 1 denotes the gelatin layer, and subscript 2 denotes the nylon layer. Note that  $\varepsilon_2$  will be 0 at all times since the resting length of the nylon layer does not change.

The moment of inertia of each layer is modeled as a solid rectangular beam using Eqn. 2.

$$I = \frac{a^3 w}{12} \quad (2)$$

The final bending angle of the bilayer can then be deter-

mined using Eqn. 3.

$$\theta = \frac{L}{\rho} \quad (3)$$

where  $L$  is the length of the bending portion of the hinge, which is the distance between the aluminum plates.

## EXPERIMENTS AND RESULTS

### Tensile Tests

We first measured the Young's modulus of the hydrogel. Test samples were made using a sandwich design. Two 200  $\mu\text{m}$



**FIGURE 4:** TENSILE TEST FOR MEASURING YOUNG'S MODULUS OF THE HYDROGEL.

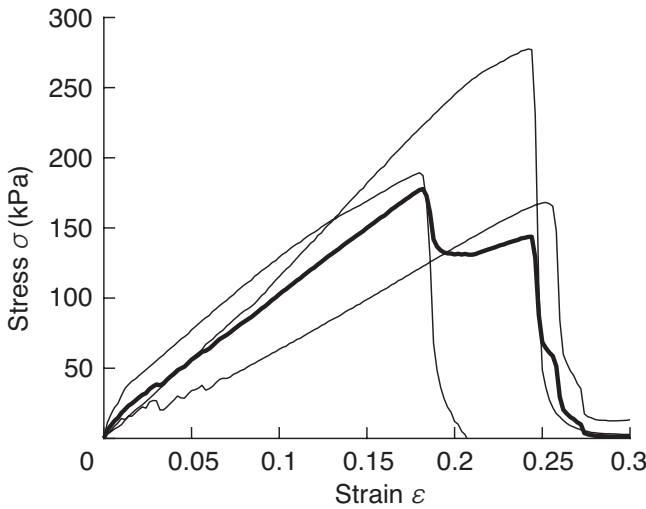


**FIGURE 5:** SRESS-STRAIN MEASUREMENTS OF THE DEHYDRATED HYDROGEL. THIN LINES REPRESENT INDIVIDUAL SAMPLES (N=3). THICK LINE REPRESENTS THE MEAN VALUE.

thick aluminum shim were used as rigid layers, with holes cut using the fiber laser cutter and used for clamping the samples to the tensile tester. The hydrogel was then sandwiched into the PDA coated aluminum shim. Test samples were clamped on a Mecmesin Multi-Test 2.5i (10N) as shown in Fig. 4.

Three samples were made under the same conditions: the hydrogels were all made with 4% crosslink, initially 3 mm thick and left in PEG for 24 hours to dehydrate. Experimental results are shown in Fig. 5, where the thin lines represent the test results for each individual sample and the thick line represents the mean value of the three tests. From the resulting curve, we found a linear relationship between the stress and the stain, which gave us an average Young's Modulus of 914.3 kPa for the dehydrated hydrogel with 4% crosslink.

#### Folding with Varying Hydrogel Thickness

A picture of the scaffold with hydrogel on top and the corresponding folding angle  $\theta$  is shown in Fig. 6. The scaffold is 20 mm wide and 10 mm long for each folding plate, with a gap of 1 mm for the flexural hinge, which is either 25  $\mu\text{m}$  or 50  $\mu\text{m}$  thick. The hydrogel is 18 mm  $\times$  18 mm with three different thicknesses: 1.5 mm, 3 mm or 4.5 mm.

Scaffolds coated with different hydrogel thicknesses were placed under a microscope (Nikon SMZ18, with Imaging Source DFK) in a rectangular vessel. The scaffolds were clamped vertically with the surfaces of the scaffolds perpendicular to the ground to eliminate the effect of gravity on the folding performance. The performance was recorded using the time-lapse

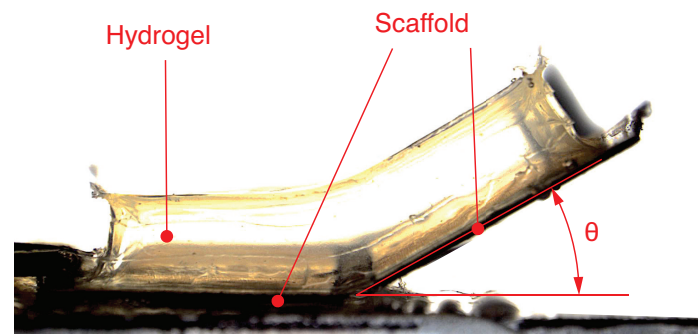


**FIGURE 6:** SELF-FOLDING HINGE.

function of the microscope, with pictures taken every 5 mins, and the position of the scaffold's rotating section was tracked using a MATLAB program. From this, the final folding angle  $\theta$  was calculated and plotted.

Hydrogels with three different thicknesses (1.5 mm, 3 mm and 4.5 mm when hydrated) were used. The thickness of the hinge was fixed to 25  $\mu\text{m}$  and the hydrogel was fixed to 4% crosslink. The final folding angles  $\theta$  with error and predicted values are plotted (Fig. 7), where gray solid bars represent the experimental final folding angle, black bars represent standard deviations and hatched bars represent the value predicted by our model. From the results, we can see the mathematical model correctly predicted the final folding angle for the scaffolds with

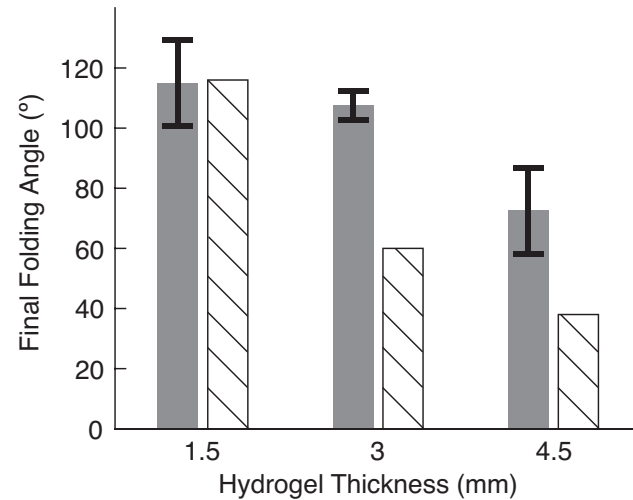


**FIGURE 7:** EXPERIMENTAL RESULTS FOR VARYING HYDROGEL THICKNESS (N = 3). GRAY SOLID: EXPERIMENTAL RESULTS; BLACK LINE: STANDARD DEVIATION; HATCHED: MODEL PREDICTION.

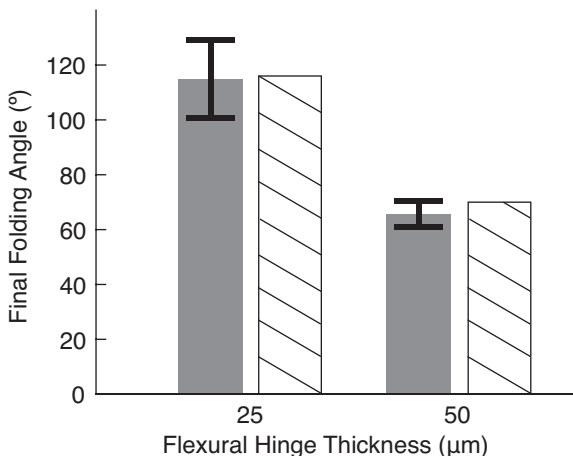


**FIGURE 8: EXPERIMENTAL RESULTS FOR VARYING HINGE THICKNESS (N = 3). GRAY SOLID: EXPERIMENTAL RESULTS; BLACK LINE: STANDARD DEVIATION; HATCHED: MODEL PREDICTION.**

a hydrogel thickness of 1.5 mm. However, the model underestimated the performance of the scaffolds with hydrogel thicknesses of 3 mm and 4.5 mm. We believe that the reason for this underestimation is the bilayer assumption only works for small displacements and breaks down for large layer thicknesses.

### Folding with Varying Hinge Thickness

Nylon films with two different thicknesses (25  $\mu\text{m}$  and 50  $\mu\text{m}$ ) were used as the flexural hinge layer. The hydrogel thickness was fixed to 1.5 mm with 4% crosslink. The final folding angle  $\theta$  was plotted with the standard deviation and predicted value (Fig. 8). For these thin hydrogels, the experimental results match our model.

### Chemo-Mechatronic System Prototype

We built a self-folding hinge with a circuit and embedded conductive trace. The dimensions are shown in Fig. 9(a). The length of the hinge was increased and the ends of each face were pre-folded to 90° so that the two plates of the hinge contact each other when folded. A copper-clad polyimide sheet (DuPont™ Pyralux® AC, AC 091200EV) was used to fabricate the conductive trace. This sheet consisted of a 9  $\mu\text{m}$  copper foil layer and a 12  $\mu\text{m}$  polyimide substrate. The circuit pattern was first masked on the copper using a solid ink printer (ColorCube 8580). Then the sheet was submerged in a copper etchant solution (UN2582 Ferric Chloride Solution, 8, PGIII). The exposed copper was dissolved in the solution and the desired circuit was left on the polyimide. This circuit was laminated on one side of the scaffold, as shown in Fig. 9(b). An LED (SSL-LX5093IT)

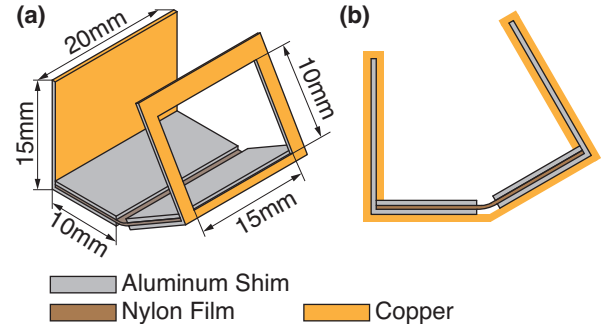


**FIGURE 9: THE SELF-FOLDING SENSOR WITH A CIRCUIT AND EMBEDDED CONDUCTIVE TRACE. (a) ISOMETRIC VIEW. (b) FRONT VIEW**

and 3 V cell battery (CR2320) were then installed, completing the circuit.

The self-folding hinge with a circuit and embedded conductive trace is shown in Fig. 10. The hinge was initially approximately flat with a folding angle  $\theta$  of 5° (Fig. 10(a)). In the presence of PEG, the hydrogel dehydrated and folded the hinge (Fig. 10(b)). Eventually, after six hours, the two ends of the hinge contacted each other when the folding angle  $\theta$  reached 60°, causing the LED to light (Fig. 10(c)). The LED remained powered until the battery died, even when PEG was removed.

### Discussion

In this paper, we have proposed and implemented a self-folding technique driven by the chemical actuation of a hydrogel. We designed and fabricated a self-folding hinge using a laminated structure with a circuit and embedded conductive trace. We also demonstrated the potential of this approach as a chemical sensor. This prototype suggests that integration of chemical and electrical systems through a mechanical medium is practical and functional.

We used a bilayer model to predict the final fold angle, but this model assumes that the bilayer thickness is much smaller than the radius of curvature. As the thickness of the hydrogel increases, the model loses its accuracy. We believe that a more complete mechanical model [30] can be used to more accurately predict the folding behavior. The mechanical behavior of the gelatin may also be nonlinear or time-dependent, especially as it dehydrates, so a more thorough mechanical analysis could explain the disparity between the model and results.

Some error in the experimental results may be caused by variation in the fabrication process. First, the mold is attached to the scaffold manually, which may induce some variation on the location where the hydrogel attaches to the scaffold. Second, the hydrogel layer has an uneven thickness because it is poured into

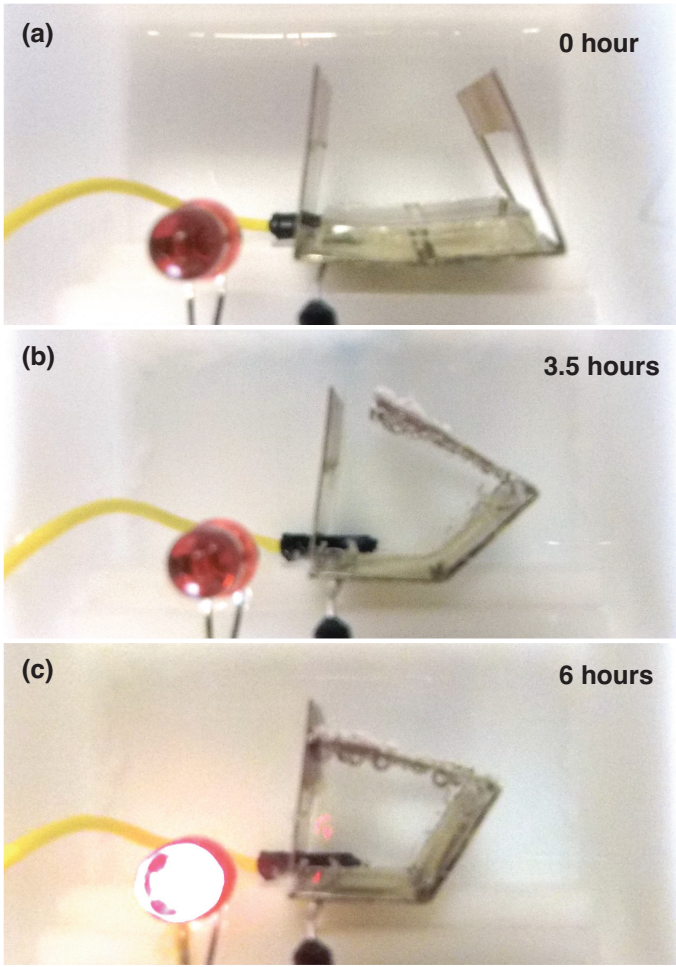


**FIGURE 10: ACTIVATION OF SELF-FOLDING SENSOR.** (a) INITIAL POSITION. (b) 3.5 HOURS INTO EXPOSURE OF PEG. (c) SIX HOURS AFTER EXPOSURE TO PEG, WHEN LED LIGHTS.

a mold. Future work will investigate how to improve fabrication precision. The minimum sensor size is also limited by our fabrication process, so in order to build micrometer-scale sensors we will need to use MEMS fabrication techniques. We expect that improving precision and miniaturizing these devices will be complementary.

This work indicates some potential avenues for future research. The hydrogel dehydrates very slowly in the presence of PEG, which leads to a long actuation time. Future efforts may be faster and more efficient if we can figure out a way to accelerate the chemical reaction. Furthermore, we constrained the crosslink to 4% in this study, but we expect that crosslinking will affect the performance of bending. Future experiments can vary the crosslink to observe this effect. Finally, it's possible to tailor hydrogels to react to particular molecules, including cancer

antigens [31]. If we can integrate these hydrogels into the device presented here, we can design it to detect specific signals. In summary, we expect that further research will improve the flexibility and practicality of this approach.

## ACKNOWLEDGMENT

The authors would like to thank the Northeastern University Tier 1 Program for funding.

## REFERENCES

- [1] Liu, C., and Felton, S. M., 2017. "A self-folding robot arm for load-bearing operations". In Intelligent Robots and Systems (IROS), 2017 IEEE/RSJ International Conference on, IEEE, pp. 1979–1986.
- [2] Malachowski, K., Jamal, M., Jin, Q., Polat, B., Morris, C. J., and Gracias, D. H., 2014. "Self-folding single cell grippers". *Nano letters*, **14**(7), pp. 4164–4170.
- [3] Nisser, M. E., Felton, S. M., Tolley, M. T., Rubenstein, M., and Wood, R. J., 2016. "Feedback-controlled self-folding of autonomous robot collectives". In Intelligent Robots and Systems (IROS), 2016 IEEE/RSJ International Conference on, IEEE, pp. 1254–1261.
- [4] Boncheva, M., Andreev, S. A., Mahadevan, L., Winkelman, A., Reichman, D. R., Prentiss, M. G., Whitesides, S., and Whitesides, G. M., 2005. "Magnetic self-assembly of three-dimensional surfaces from planar sheets". *Proceedings of the National Academy of Sciences of the United States of America*, **102**(11), pp. 3924–3929.
- [5] Huang, H.-W., Sakar, M. S., Petruska, A. J., Pané, S., and Nelson, B. J., 2016. "Soft micromachines with programmable motility and morphology". *Nature communications*, **7**, p. 12263.
- [6] Miyashita, S., Guitron, S., Li, S., and Rus, D., 2017. "Robotic metamorphosis by origami exoskeletons". *Science Robotics*.
- [7] Liu, Y., Boyles, J. K., Genzer, J., and Dickey, M. D., 2012. "Self-folding of polymer sheets using local light absorption". *Soft Matter*, **8**(6), pp. 1764–1769.
- [8] Felton, S. M., Tolley, M. T., Shin, B., Onal, C. D., Demaine, E. D., Rus, D., and Wood, R. J., 2013. "Self-folding with shape memory composites". *Soft Matter*, **9**(32), pp. 7688–7694.
- [9] Yoshida, E., Murata, S., Kokaji, S., Tomita, K., and Kurokawa, H., 2000. "Micro self-reconfigurable robotic system using shape memory alloy". In *Distributed autonomous robotic systems 4*. Springer, pp. 145–154.
- [10] Paik, J. K., Hawkes, E., and Wood, R. J., 2010. "A novel low-profile shape memory alloy torsional actuator". *Smart Materials and Structures*, **19**(12), p. 125014.

- [11] Bertagne, C., Walgren, P., Erickson, L., Sheth, R., Whitcomb, J., and Hartl, D. J., 2018. “Coupled behavior of shape memory alloy-based morphing spacecraft radiators: Experimental assessment and analysis”. *Smart Materials and Structures*.
- [12] Chemisky, Y., Hartl, D. J., and Meraghni, F., 2018. “Three-dimensional constitutive model for structural and functional fatigue of shape memory alloy actuators”. *International Journal of Fatigue*.
- [13] Bertagne, C. L., Cognata, T. J., Sheth, R. B., Dinsmore, C. E., and Hartl, D. J., 2017. “Testing and analysis of a morphing radiator concept for thermal control of crewed space vehicles”. *Applied Thermal Engineering*, **124**, pp. 986–1002.
- [14] Niiyama, R., Sun, X., Sung, C., An, B., Rus, D., and Kim, S., 2015. “Pouch motors: Printable soft actuators integrated with computational design”. *Soft Robotics*, **2**(2), pp. 59–70.
- [15] Sun, X., Felton, S. M., Niiyama, R., Wood, R. J., and Kim, S., 2015. “Self-folding and self-actuating robots: A pneumatic approach”. In *Robotics and Automation (ICRA), 2015 IEEE International Conference on*, IEEE, pp. 3160–3165.
- [16] Guan, J., He, H., Hansford, D. J., and Lee, L. J., 2005. “Self-folding of three-dimensional hydrogel microstructures”. *The Journal of Physical Chemistry B*, **109**(49), pp. 23134–23137.
- [17] Ahmed, E. M., 2015. “Hydrogel: Preparation, characterization, and applications: A review”. *Journal of advanced research*, **6**(2), pp. 105–121.
- [18] Ionov, L., 2014. “Hydrogel-based actuators: possibilities and limitations”. *Materials Today*, **17**(10), pp. 494–503.
- [19] Holback, H., Yeo, Y., and Park, K., 2011. “Hydrogel swelling behavior and its biomedical applications”. In *Biomedical Hydrogels*. Elsevier, pp. 3–24.
- [20] Kobayashi, K., Oh, S. H., Yoon, C., and Gracias, D. H., 2017. “Multitemperature responsive self-folding soft biomimetic structures”. *Macromolecular rapid communications*.
- [21] Cangialosi, A., Yoon, C., Liu, J., Huang, Q., Guo, J., Nguyen, T. D., Gracias, D. H., and Schulman, R., 2017. “Dna sequence-directed shape change of photopatterned hydrogels via high-degree swelling”. *Science*, **357**(6356), pp. 1126–1130.
- [22] Hoare, T. R., and Kohane, D. S., 2008. “Hydrogels in drug delivery: Progress and challenges”. *Polymer*, **49**(8), pp. 1993–2007.
- [23] Djagny, K. B., Wang, Z., and Xu, S., 2001. “Gelatin: a valuable protein for food and pharmaceutical industries”. *Critical reviews in food science and nutrition*, **41**(6), pp. 481–492.
- [24] Yang, G., Xiao, Z., Ren, X., Long, H., Qian, H., Ma, K., and Guo, Y., 2016. “Enzymatically crosslinked gelatin hydrogel promotes the proliferation of adipose tissue-derived stromal cells”. *PeerJ*, **4**, p. e2497.
- [25] Balakrishnan, B., Joshi, N., Jayakrishnan, A., and Banerjee, R., 2014. “Self-crosslinked oxidized alginate/gelatin hydrogel as injectable, adhesive biomimetic scaffolds for cartilage regeneration”. *Acta biomaterialia*, **10**(8), pp. 3650–3663.
- [26] Ding, Y., Floren, M., and Tan, W., 2016. “Mussel-inspired polydopamine for bio-surface functionalization”. *Biosurface and Biotribology*, **2**(4), pp. 121–136.
- [27] Mallinson, D., Mullen, A. B., and Lamprou, D. A., 2018. “Probing polydopamine adhesion to protein and polymer films: microscopic and spectroscopic evaluation”. *Journal of Materials Science*, **53**(5), pp. 3198–3209.
- [28] Yung, C., Wu, L., Tullman, J., Payne, G., Bentley, W., and Barbari, T., 2007. “Transglutaminase crosslinked gelatin as a tissue engineering scaffold”. *Journal of Biomedical Materials Research Part A*, **83**(4), pp. 1039–1046.
- [29] Timoshenko, S., 1925. “Analysis of bi-metal thermostats”. *JOSA*, **11**(3), pp. 233–255.
- [30] Alford, P. W., Feinberg, A. W., Sheehy, S. P., and Parker, K. K., 2010. “Biohybrid thin films for measuring contractility in engineered cardiovascular muscle”. *Biomaterials*, **31**(13), pp. 3613–3621.
- [31] Bencherif, S. A., Sands, R. W., Ali, O. A., Li, W. A., Lewin, S. A., Braschler, T. M., Shih, T.-Y., Verbeke, C. S., Bhatta, D., Dranoff, G., et al., 2015. “Injectable cryogel-based whole-cell cancer vaccines”. *Nature communications*, **6**, p. 7556.